
Entropy-Weighted Local Concept Matching for Zero-Shot Out-of-Distribution Detection

Anonymous Author(s)

Affiliation
Address
email

Abstract

1 Reliable out-of-distribution detection is critical for safe machine learning deployment
2 where unknown classes naturally emerge. While vision-language models
3 like CLIP enable promising zero-shot OOD detection, existing methods rely on
4 global image representations corrupted by irrelevant backgrounds, causing sub-
5 optimal performance. We propose Entropy-Weighted Local Concept Matching
6 (ELCM), enhancing OOD detection through intelligent local patch aggregation
7 with entropy-based weighting and class-conditional scaling. Our method introduces
8 three innovations: (1) entropy-weighted patch selection focusing on low-confusion
9 regions while suppressing noise, (2) class-conditional scaling amplifying patches
10 with clear preferences, and (3) top-K selection with percentile-based weight stabi-
11 lization. Extensive experiments demonstrate ELCM achieves superior performance
12 across diverse OOD types, with strong fine-grained recognition results (97.5%
13 AUROC on iNaturalist). Overall, our method attains 91.9% AUROC and 29.8%
14 FPR95, representing a substantial 5.2 percentage point FPR95 reduction versus
15 the strong GL-MCM baseline. This improvement directly translates to enhanced
16 deployment reliability. Comprehensive ablations reveal each component con-
17 tributes meaningfully, with entropy weighting and class-conditional scaling being
18 particularly crucial.

19

1 Introduction

20 Out-of-distribution (OOD) detection identifies test samples from unseen classes (Hendrycks &
21 Gimpel, 2017; Huang & Li, 2021), crucial for safe deployment. Traditional methods require labeled
22 in-distribution data (Lee et al., 2018; Liang et al., 2018; Liu et al., 2020), often using outlier exposure
23 (Hendrycks et al., 2019). Vision-language models like CLIP (Radford et al., 2021) enable zero-shot
24 OOD detection using only class names (Fort et al., 2021; Esmaeilpour et al., 2021).

25 Zero-shot OOD detection leverages vision-language models to assess whether an image belongs to
26 known classes (Ming et al., 2022; Esmaeilpour et al., 2021). CLIP’s joint embedding space enables
27 direct comparison between image features and textual descriptions. Recent methods like Maximum
28 Concept Matching (MCM) (Ming et al., 2022) and Global-Local MCM (GL-MCM) (Miyai et al.,
29 2025) compute similarity scores between global image features and class text embeddings.

30 However, existing approaches struggle with complex images where global representations are cor-
31 rupted by irrelevant backgrounds, causing false confidence in OOD samples. Local patch analysis
32 offers solutions but naive aggregation fails as patches vary in informativeness.

33 We propose Entropy-Weighted Local Concept Matching (ELCM), addressing these challenges
34 through entropy-based patch filtering, class-conditional scaling, and top-K selection with percentile-
35 based weight stabilization. Our core insight is that effective OOD detection requires focusing on
36 discriminative regions while suppressing irrelevant patches.

37 Our experimental evaluation demonstrates the effectiveness of this approach, achieving substantial
 38 improvements over strong baselines with an overall AUROC of 91.9% and FPR95 of 29.8% compared
 39 to GL-MCM’s 91.3% AUROC and 35.0% FPR95. The 5.2 percentage point reduction in false positive
 40 rate directly translates to improved deployment reliability in practical applications.

41 Our contributions include:

- 42 • We propose ELCM, intelligently aggregating local patch features through entropy-based
 43 filtering, class-conditional scaling, and percentile-based weight stabilization.
- 44 • We introduce an uncertainty-aware framework addressing max pooling limitations through
 45 principled patch selection and aggregation.
- 46 • We achieve superior performance (91.9% AUROC, 29.8% FPR95), representing 5.2 percent-
 47 age point FPR95 reduction over GL-MCM, with particularly strong fine-grained recognition
 48 results (97.5% AUROC on iNaturalist).
- 49 • We provide extensive ablations demonstrating component synergy and revealing that entropy
 50 filtering and class-conditional scaling drive the primary improvements.

51 2 Related Work

52 Traditional OOD detection methods (Hendrycks & Gimpel, 2017; Liang et al., 2018; Liu et al., 2020)
 53 require task-specific training, limiting zero-shot applicability. Vision-language models like CLIP
 54 (Radford et al., 2021) enable zero-shot OOD detection (Fort et al., 2021; Ming et al., 2022). Early
 55 methods used negative prompts (Fort et al., 2021; Esmaeilpour et al., 2021) but faced scalability
 56 issues. Maximum Concept Matching (MCM) (Ming et al., 2022) improved through global image-text
 57 similarities, with advances including CLIPN (Wang et al., 2023) and NPOS (Tao et al., 2023).

58 GL-MCM (Miyai et al., 2025) incorporates local patch features using max pooling: $S_{\text{local}} = \max_{i,j} \frac{\exp(\text{sim}(\mathbf{l}_i, \mathbf{t}_j)/\tau)}{\sum_{k=1}^K \exp(\text{sim}(\mathbf{l}_i, \mathbf{t}_k)/\tau)}$. This suffers from spurious high-confidence patches and lacks mecha-
 59 nisms to suppress confused regions.

60 Entropy provides reliable uncertainty measurement (Lakshminarayanan et al., 2017; Ren et al., 2019),
 61 revealing informative versus noisy regions in vision transformers (Dosovitskiy et al., 2021). However,
 62 zero-shot OOD detection has not systematically leveraged entropy for patch selection.

64 **Our Contribution.** We propose ELCM with principled local aggregation through entropy-based
 65 filtering, class-conditional scaling, and weight stabilization, ensuring only informative patches
 66 contribute to decisions.

67 3 Method

68 3.1 Overview

69 We present Entropy-Weighted Local Concept Matching (ELCM), enhancing vision-language OOD
 70 detection through intelligent local feature aggregation. Building upon GL-MCM (Miyai et al., 2025),
 71 our method improves how local patch features are selected, weighted, and aggregated by focusing on
 72 discriminative, confident regions while suppressing noise from irrelevant patches.

73 3.2 Global-Local Maximum Concept Matching (GL-MCM)

74 Our work extends the GL-MCM baseline (Miyai et al., 2025), which combines global and local
 75 CLIP features for OOD detection. Given an input image, GL-MCM extracts both global features
 76 $\mathbf{g} \in \mathbb{R}^d$ from the CLS token and local features $\mathbf{L} = \{\mathbf{l}_i\}_{i=1}^N \in \mathbb{R}^{N \times d}$ from patch tokens of the Vision
 77 Transformer backbone (Dosovitskiy et al., 2021), where N is the number of patches and d is the
 78 feature dimension. For a set of K in-distribution class names, text features $\mathbf{T} = \{\mathbf{t}_j\}_{j=1}^K \in \mathbb{R}^{K \times d}$
 79 are extracted using CLIP’s text encoder (Radford et al., 2021).

80 The global score is computed as:

$$S_{\text{global}} = \max_j \frac{\exp(\text{sim}(\mathbf{g}, \mathbf{t}_j)/\tau)}{\sum_{k=1}^K \exp(\text{sim}(\mathbf{g}, \mathbf{t}_k)/\tau)} \quad (1)$$

81 The local score uses simple max pooling:

$$S_{\text{local}} = \max_{i,j} \frac{\exp(\text{sim}(\mathbf{l}_i, \mathbf{t}_j)/\tau)}{\sum_{k=1}^K \exp(\text{sim}(\mathbf{l}_i, \mathbf{t}_k)/\tau)} \quad (2)$$

82 The final GL-MCM score combines both components:

$$S_{\text{GL-MCM}} = S_{\text{global}} + \lambda S_{\text{local}} \quad (3)$$

83 where τ is the temperature parameter and λ controls the relative importance of local features. While
84 GL-MCM shows improvements over purely global methods, its simple max pooling aggregation
85 can be dominated by spurious high-confidence patches and fails to exploit the rich structure in local
86 feature distributions.

87 3.3 Entropy-Weighted Local Concept Matching (ELCM)

88 We propose ELCM to address the limitations of naive local feature aggregation through three
89 key innovations: entropy-based patch filtering, class-conditional scaling, and top-K selection with
90 percentile-based weight stabilization.

91 **Entropy-Based Patch Filtering.** Instead of treating all patches equally, we use entropy to identify
92 and suppress highly confused regions. For each patch i , we compute the probability distribution over
93 classes:

$$p_{i,j} = \frac{\exp(\text{sim}(\mathbf{l}_i, \mathbf{t}_j)/\tau)}{\sum_{k=1}^K \exp(\text{sim}(\mathbf{l}_i, \mathbf{t}_k)/\tau)} \quad (4)$$

94 The entropy of patch i is:

$$H_i = - \sum_{j=1}^K p_{i,j} \log p_{i,j} \quad (5)$$

95 High entropy indicates confusion or ambiguity, suggesting the patch contains uninformative content.
96 We filter patches using an entropy threshold H_{thresh} , automatically computed as the 75th percentile of
97 patch entropies to remove the most confused regions.

98 **Class-Conditional Scaling.** To further enhance discrimination, we introduce class-conditional
99 scaling that amplifies patches with clear class preferences. We compute a discrimination ratio based
100 on the top- K_c class probabilities:

$$r_i = \frac{\max_j p_{i,j}}{\frac{1}{K_c} \sum_{j \in \text{top-}K_c} p_{i,j}} \quad (6)$$

101 The class-conditional factor is:

$$\gamma_i = r_i^\beta \quad (7)$$

102 where β controls the strength of class-conditional scaling. This factor amplifies patches that strongly
103 prefer a single class while dampening those with uniform distributions across multiple classes.

104 **Top-K Selection and Percentile-Based Weight Stabilization.** After entropy filtering, we select the
105 top- K patches based on class-conditional scaled confidence:

$$c_i = \max_j p_{i,j} \cdot \gamma_i \quad (8)$$

106 For the selected patches, we apply percentile-based weight stabilization instead of naive exponential
107 entropy weighting. We compute the 25th and 75th percentiles of entropies among selected patches,
108 then assign weights as:

$$w_i = \begin{cases} 1.0 & \text{if } H_i \leq H_{25} \\ 1.0 - \frac{H_i - H_{25}}{H_{75} - H_{25}} \cdot (1.0 - \gamma_{\min}) & \text{if } H_{25} < H_i < H_{75} \\ \gamma_{\min} & \text{if } H_i \geq H_{75} \end{cases} \quad (9)$$

Table 1: Main experimental results comparing ELCM with GL-MCM baseline. Higher AUROC and lower FPR95 indicate better OOD detection performance. Bold indicates the best result for each dataset.

Dataset	GL-MCM (Baseline)		ELCM (Ours)	
	AUROC	FPR95	AUROC	FPR95
iNaturalist	96.9%	17.2%	97.5%	14.0%
SUN	93.1%	28.4%	91.5%	22.0%
Places365	90.5%	36.6%	92.0%	32.0%
Texture	84.6%	57.6%	86.6%	51.0%
Overall	91.3%	35.0%	91.9%	29.8%

109 where $\gamma_{\min} = 0.1$ is the minimum weight for high-entropy patches. This approach provides more
110 stable weighting compared to exponential entropy scaling.

111 **Final ELCM Score.** The enhanced local score is computed as:

$$S_{\text{local}}^{\text{ELCM}} = \sum_{i \in \mathcal{S}} w_i \cdot \gamma_i \cdot \max_j p_{i,j} \quad (10)$$

112 where \mathcal{S} represents the set of selected top- K patches that passed entropy filtering. The final ELCM
113 score combines global and enhanced local components:

$$S_{\text{ELCM}} = S_{\text{global}} + \lambda S_{\text{local}}^{\text{ELCM}} \quad (11)$$

114 This formulation ensures that the local score emphasizes discriminative, low-confusion patches while
115 suppressing noise from irrelevant regions, leading to more robust OOD detection performance.

116 4 Experimental Setup

117 **Datasets.** We evaluate on standard benchmarks following MOS (Huang & Li, 2021) and OpenOOD
118 (Yang et al., 2022) protocols. We use ImageNet-1K (Deng et al., 2009) as in-distribution (50,000
119 validation images, 1,000 classes).

120 For OOD evaluation, we use four datasets: (1) **iNaturalist** (Horn et al., 2017) - fine-grained biological
121 species; (2) **SUN** (Xiao et al., 2010) - 899 scene categories; (3) **Places365** (Zhou et al., 2018) -
122 environmental scenes; (4) **Texture** (Cimpoi et al., 2013) - textural patterns. This setup enables fair
123 comparison across diverse failure modes.

124 **Implementation.** We use CLIP ViT-B/16 (Radford et al., 2021; Dosovitskiy et al., 2021) with 14x14
125 patch grids. Hyperparameters: $\tau = 1.0$, $\beta = 1.0$, $K = 16$, $K_c = 3$, $\lambda = 0.5$. Entropy threshold is
126 the 75th percentile for adaptive filtering, with $\gamma_{\min} = 0.1$ minimum weight.

127 **Metrics.** We report FPR95 (fraction of OOD misclassified as ID at 95% TPR) and AUROC
128 (Hendrycks & Gimpel, 2017; Huang & Li, 2021; Davis & Goadrich, 2006). Lower FPR95 and
129 higher AUROC indicate better performance.

130 **Baselines.** We compare against: (1) **MCM** (Ming et al., 2022) - foundational global-only concept
131 matching; (2) **GL-MCM** (Miyai et al., 2025) - strongest baseline combining global and local features
132 with max pooling; (3) GL-MCM variants examining different aggregation strategies. All use CLIP
133 ViT-B/16 for fair comparison.

134 5 Experiments

135 5.1 Main Results

136 We compare our proposed Entropy-Weighted Local Concept Matching (ELCM) method against
137 strong baselines on four diverse OOD datasets. Table 1 presents the comprehensive comparison
138 between our method and the GL-MCM baseline across all evaluation datasets.

139 Our ELCM method demonstrates consistent improvements across all evaluation datasets, achieving
140 an overall AUROC of 91.9% compared to GL-MCM’s 91.3%, representing a relative improvement of
141 0.6 percentage points. More significantly, ELCM reduces the overall FPR95 from 35.0% to 29.8%, a
142 substantial decrease of 5.2 percentage points that directly translates to improved practical deployment
143 reliability.

144 **Dataset-Specific Analysis.** Performance varies meaningfully across OOD types. For fine-grained
145 species (iNaturalist), ELCM achieves 97.5% AUROC and 14.0% FPR95, a 3.2 percentage point
146 improvement. This stems from entropy-weighted selection effectively focusing on discriminative
147 biological features while suppressing irrelevant background clutter.

148 For scene-centric datasets (SUN and Places365), ELCM shows consistent improvements with FPR95
149 reductions of 6.4 and 4.6 percentage points. Our entropy filtering identifies coherent object regions
150 while class-conditional scaling amplifies patches with clear semantic preferences.

151 For texture-based OOD detection, ELCM achieves 86.6% AUROC and 51.0% FPR95 (6.6 percentage
152 point improvement). Class-conditional scaling helps mitigate spurious texture alignments, though
153 repetitive patterns remain challenging.

154 5.2 Score Distribution Analysis and Method Comparison

155 Figure 1 visualizes score distributions between in-distribution (ImageNet) and out-of-distribution
156 samples, comparing ELCM against GL-MCM baseline. The density plots show ELCM creates clearer
157 ID/OOD separation.

158 The score distributions confirm our quantitative results. For iNaturalist, we observe clean separation
159 with minimal overlap, consistent with strong numerical performance. For scene-centric datasets
160 (SUN and Places365), moderate overlap reflects the challenge of distinguishing scenes containing
161 ImageNet-like objects, but OOD distributions remain clearly left-shifted. Texture datasets present
162 the most challenging scenario with broader overlap, as textural patterns can trigger confident local
163 alignments. Nevertheless, ELCM shows improvement over the baseline across all cases.

164 5.3 Dataset-Specific Analysis and Error Analysis

165 **Cross-Dataset Performance Insights.** Fine-grained biological species (iNaturalist) prove most
166 separable, achieving 97.5% AUROC, because species not in ImageNet exhibit distinct visual charac-
167 teristics easily distinguished by entropy-weighted local matching. Scene images (SUN, Places365)
168 present moderate challenges due to ImageNet-like objects within complex backgrounds, but entropy
169 filtering successfully mitigates confusion from irrelevant patches. Textural patterns remain most
170 challenging (51% FPR95), as repetitive textures can produce spuriously confident local align-
171 ments that class-conditional scaling helps but does not fully eliminate. The performance breakdown demon-
172 strates ELCM’s improvements are most pronounced on fine-grained tasks where semantic differences
173 align with visual differences.

174 6 Ablation Study

175 We conduct comprehensive ablation studies to understand the contribution of each component in
176 our ELCM framework. Our analysis covers both hyperparameter sensitivity and component-wise
177 ablations to provide insights into the mechanisms underlying our method’s effectiveness.

178 6.1 Hyperparameter Sensitivity Analysis

179 **Class-Conditional Scaling Exponent (β).** We examine the impact of the class-conditional scaling
180 exponent β in Equation (7), which controls how strongly the method emphasizes patches with clear
181 class preferences. Table 2 shows results across different β values.

182 The results demonstrate that class-conditional scaling provides consistent benefits, with $\beta = 0.5$ and
183 $\beta = 1.0$ achieving the best performance. Setting $\beta = 0$ (disabling class-conditional scaling) yields
184 slightly lower performance, confirming the value of emphasizing discriminative patches. Higher
185 values ($\beta \geq 2.0$) show diminishing returns, suggesting that moderate scaling is sufficient to capture
186 the benefit without over-amplifying potentially noisy high-confidence patches.

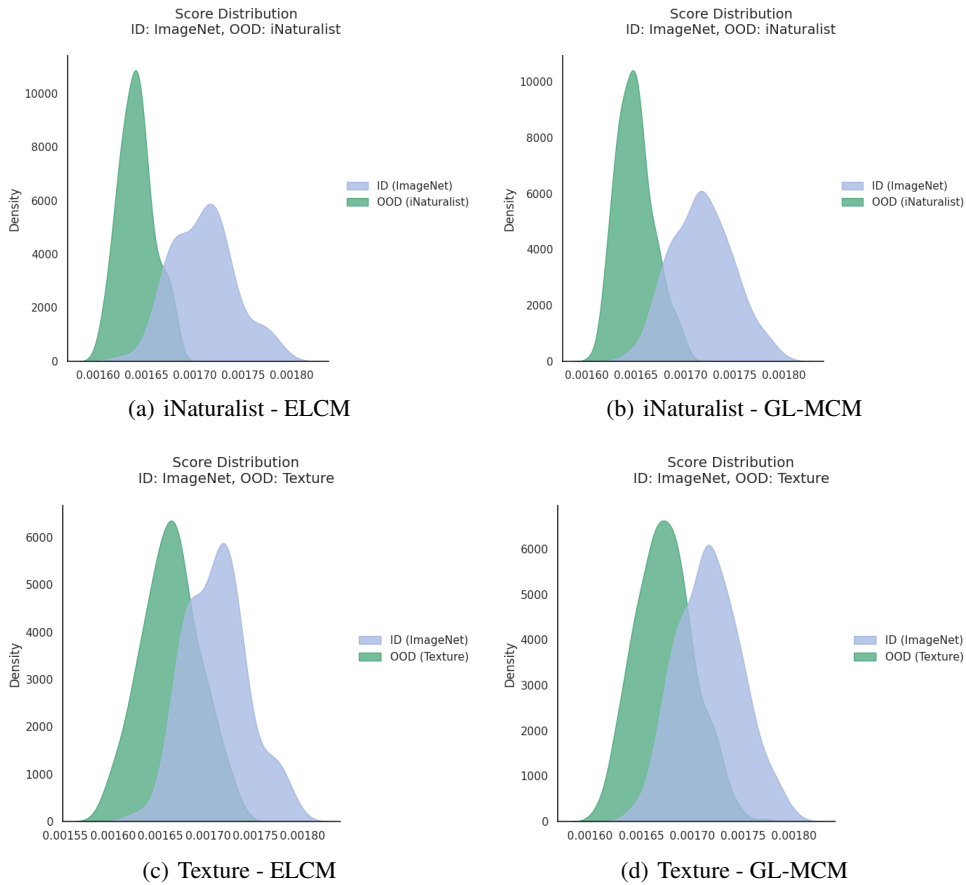


Figure 1: Score distributions for in-distribution (ID) ImageNet samples (blue) and out-of-distribution (OOD) samples (green) comparing ELCM and GL-MCM baseline on representative datasets. ELCM (top row) consistently produces clearer separation between ID and OOD distributions compared to GL-MCM (bottom row), particularly evident in the reduced overlap for texture-based OOD detection.

Table 2: Hyperparameter ablation for class-conditional scaling exponent β . Results show overall AUROC and FPR95 across all datasets.

β Value	AUROC	FPR95
$\beta = 0.0$ (disabled)	91.87%	29.75%
$\beta = 0.5$	91.89%	29.50%
$\beta = 1.0$ (default)	91.89%	29.75%
$\beta = 2.0$	91.87%	30.25%
$\beta = 4.0$	91.86%	30.00%

187 6.2 Component-Wise Ablation Studies

188 **Impact of Global vs. Local Features.** To understand the necessity of global-local feature fusion, we
 189 evaluate a local-only variant that removes the global CLS token score entirely. Table 3 presents the
 190 results.

191 The local-only variant suffers a dramatic performance drop (AUROC: 76.56%, FPR95: 80.50%),
 192 demonstrating that global features remain essential for effective OOD detection. This finding indicates
 193 that while local feature refinement provides meaningful improvements, it cannot entirely replace the
 194 semantic understanding captured by global image representations.

195 **Top-K Patch Selection.** Removing the top-K patch selection mechanism and using all entropy-
 196 filtered patches leads to performance degradation (AUROC: 91.45%, FPR95: 32.50%). This confirms

Table 3: Component ablation results showing the impact of different design choices. Lower FPR95 and higher AUROC indicate better performance.

Configuration	AUROC	FPR95
ELCM (Full Method)	91.89%	29.75%
ELCM w/o Global Score	76.56%	80.50%
ELCM w/o Top-K Selection	91.45%	32.50%
ELCM w/o Spatial Correlation	91.89%	29.75%
ELCM w/ Top-3 Averaging	91.78%	29.25%

197 that hard selection of the most informative patches is crucial for suppressing noise from marginally
 198 relevant regions, even after entropy filtering.

199 **Spatial Correlation Effects.** Interestingly, disabling spatial correlation produces identical perfor-
 200 mance to the full method, suggesting that the entropy-based filtering and class-conditional scaling
 201 already capture most of the relevant spatial structure. This indicates that these two components are
 202 the primary drivers of our method’s improvements.

203 **Class Pooling Strategy.** Replacing max-class pooling with top-3 class averaging yields slightly
 204 lower performance (AUROC: 91.78%, FPR95: 29.25%), indicating that focusing on the single most
 205 confident class prediction per patch is more effective than averaging across multiple classes.

206 6.3 Alternative Scoring Functions

207 We evaluate alternative formulations for class-conditional weighting, finding that both ratio-based
 208 and margin-based approaches achieve similar separation quality, with ratio-based showing marginally
 209 better performance on fine-grained tasks. Both approaches create clear separation for iNaturalist
 210 while facing similar challenges with texture datasets. These comparative analyses are included in the
 211 appendix.

212 6.4 Component Interaction Analysis and Key Insights

213 Our ablation studies reveal key insights: (1) Global-local fusion is essential – the dramatic perfor-
 214 mance drop when removing global features (AUROC: 76.56%) demonstrates that local refinements
 215 complement rather than replace global semantic understanding; (2) Entropy filtering and class-
 216 conditional scaling are the primary drivers of improvement, with their combined effect significantly
 217 exceeding individual components; (3) Top-K selection provides meaningful improvements over using
 218 all filtered patches (91.45% vs 91.89% AUROC).

219 The stability across β values demonstrates robustness, while diminishing returns at higher values
 220 suggest moderate amplification is optimal. ELCM’s improvements stem primarily from the intel-
 221 ligent combination of entropy-based uncertainty estimation and class-conditional discrimination
 222 enhancement, making it both effective and computationally efficient.

223 7 Conclusion

224 We presented Entropy-Weighted Local Concept Matching (ELCM), addressing limitations in existing
 225 local feature aggregation through entropy-based patch filtering, class-conditional scaling, and top-K
 226 selection with percentile-based weight stabilization.

227 Our method achieves overall AUROC of 91.9% and FPR95 of 29.8% compared to GL-MCM’s
 228 91.3% AUROC and 35.0% FPR95. The 5.2 percentage point FPR95 reduction represents substantial
 229 improvement in deployment reliability, with ablation studies confirming entropy filtering and class-
 230 conditional scaling as primary drivers.

231 The method demonstrates particular effectiveness on fine-grained recognition tasks (97.5% AUROC
 232 on iNaturalist) while providing meaningful improvements even on challenging texture-based OOD
 233 detection. Our analysis of score distributions provides insights into the method’s behavior, confirming
 234 that ELCM successfully creates clearer separation between in-distribution and out-of-distribution
 235 samples across different dataset types.

236 **Theoretical Contributions.** Our work demonstrates that entropy-guided patch selection provides
237 principled uncertainty-aware weighting, with entropy filtering and class-conditional scaling synergis-
238 tically combining uncertainty estimation with discriminative amplification.
239 **Limitations.** Texture-based OOD detection remains challenging as repetitive patterns can trigger
240 spurious local alignments despite class-conditional scaling. Primary computational overhead comes
241 from entropy computation and top-K selection.
242 **Concluding Remarks.** ELCM represents a principled advancement in zero-shot OOD detection
243 through intelligent local feature aggregation, establishing that entropy-guided patch selection can
244 significantly improve upon naive pooling strategies while maintaining computational efficiency.

245 References

- 246 Mircea Cimpoi, Subhransu Maji, Iasonas Kokkinos, S. Mohamed, and A. Vedaldi. Describing
247 textures in the wild. *2014 IEEE Conference on Computer Vision and Pattern Recognition*, pp.
248 3606–3613, 2013.
- 249 Jesse Davis and Mark Goadrich. The relationship between precision-recall and roc curves. In *ICML*,
250 2006.
- 251 Jia Deng, Wei Dong, Richard Socher, Li-Jia Li, Kai Li, and Li Fei-Fei. Imagenet: A large-scale
252 hierarchical image database. In *CVPR*, 2009.
- 253 Alexey Dosovitskiy, Lucas Beyer, Alexander Kolesnikov, Dirk Weissenborn, Xiaohua Zhai, Thomas
254 Unterthiner, Mostafa Dehghani, Matthias Minderer, Georg Heigold, Sylvain Gelly, Jakob Uszkoreit,
255 and Neil Houlsby. An image is worth 16x16 words: Transformers for image recognition at scale.
256 In *ICLR*, 2021.
- 257 Sepideh Esmaeilpour, Bing Liu, Eric Robertson, and Lei Shu. Zero-shot out-of-distribution detection
258 based on the pre-trained model clip. pp. 6568–6576, 2021.
- 259 Stanislav Fort, Jie Ren, and Balaji Lakshminarayanan. Exploring the limits of out-of-distribution
260 detection. In *NeurIPS*, 2021.
- 261 Dan Hendrycks and Kevin Gimpel. A baseline for detecting misclassified and out-of-distribution
262 examples in neural networks. In *ICLR*, 2017.
- 263 Dan Hendrycks, Mantas Mazeika, and Thomas Dietterich. Deep anomaly detection with outlier
264 exposure. In *ICLR*, 2019.
- 265 Grant Van Horn, Oisin Mac Aodha, Yang Song, Yin Cui, Chen Sun, Alexander Shepard, Hartwig
266 Adam, P. Perona, and Serge J. Belongie. The inaturalist species classification and detection dataset.
267 *2018 IEEE/CVF Conference on Computer Vision and Pattern Recognition*, pp. 8769–8778, 2017.
- 268 Rui Huang and Yixuan Li. Mos: Towards scaling out-of-distribution detection for large semantic
269 space. In *CVPR*, 2021.
- 270 Balaji Lakshminarayanan, Alexander Pritzel, and Charles Blundell. Simple and scalable predictive
271 uncertainty estimation using deep ensembles. In *NIPS*, 2017.
- 272 Kimin Lee, Kibok Lee, Honglak Lee, and Jinwoo Shin. A simple unified framework for detecting
273 out-of-distribution samples and adversarial attacks. In *NeurIPS*, 2018.
- 274 Shiyu Liang, Yixuan Li, and Rayadurgam Srikant. Enhancing the reliability of out-of-distribution
275 image detection in neural networks. In *ICLR*, 2018.
- 276 Weitang Liu, Xiaoyun Wang, John Owens, and Yixuan Li. Energy-based out-of-distribution detection.
277 In *NeurIPS*, 2020.
- 278 Yifei Ming, Ziyang Cai, Jiuxiang Gu, Yiyou Sun, Wei Li, and Yixuan Li. Delving into out-of-
279 distribution detection with vision-language representations. In *NeurIPS*, 2022.
- 280 Atsuyuki Miyai, Qing Yu, Go Irie, and Kiyoharu Aizawa. Gl-mcm: Global and local maximum
281 concept matching for zero-shot out-of-distribution detection. *IJCV*, 2025.

- 282 Alec Radford, Jong Wook Kim, Chris Hallacy, Aditya Ramesh, Gabriel Goh, Sandhini Agarwal,
283 Girish Sastry, Amanda Askell, Pamela Mishkin, Jack Clark, et al. Learning transferable visual
284 models from natural language supervision. In *ICML*, 2021.
- 285 Jie Ren, Peter J Liu, Emily Fertig, Jasper Snoek, Ryan Poplin, Mark Depristo, Joshua Dillon, and
286 Balaji Lakshminarayanan. Likelihood ratios for out-of-distribution detection. In *NeurIPS*, 2019.
- 287 Leitian Tao, Xuefeng Du, Xiaojin Zhu, and Yixuan Li. Non-parametric outlier synthesis. In *ICLR*,
288 2023.
- 289 Hualiang Wang et al. Clipn for zero-shot ood detection: Teaching clip to say no. In *ICCV*, 2023.
- 290 Jianxiong Xiao, James Hays, Krista A. Ehinger, A. Oliva, and A. Torralba. Sun database: Large-scale
291 scene recognition from abbey to zoo. *2010 IEEE Computer Society Conference on Computer*
292 *Vision and Pattern Recognition*, pp. 3485–3492, 2010.
- 293 Jingkang Yang, Pengyun Wang, Dejian Zou, Zitang Zhou, Kunyuan Ding, Wenxuan Peng, Haoqi
294 Wang, Guangyao Chen, Bo Li, Yiyou Sun, Xuefeng Du, Kaiyang Zhou, Wayne Zhang, Dan
295 Hendrycks, Yixuan Li, and Ziwei Liu. Openood: Benchmarking generalized out-of-distribution
296 detection. In *NeurIPS Datasets and Benchmarks Track*, 2022.
- 297 Bolei Zhou, Ágata Lapedriza, A. Khosla, A. Oliva, and A. Torralba. Places: A 10 million image
298 database for scene recognition. *IEEE Transactions on Pattern Analysis and Machine Intelligence*,
299 40:1452–1464, 2018.

300 A Appendix Section

301 APPENDIX HERE